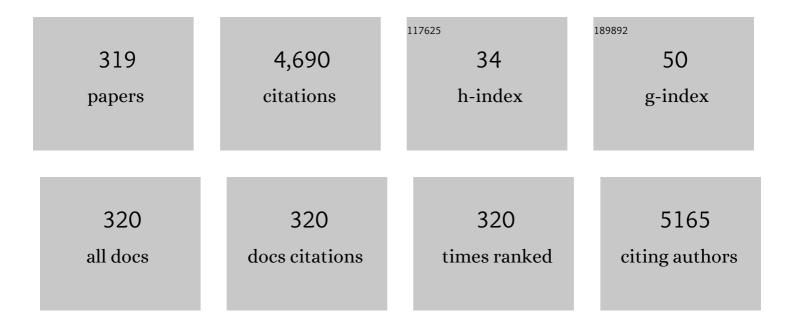
List of Publications by Year in descending order

Source: https://exaly.com/author-pdf/1373492/publications.pdf Version: 2024-02-01



VN FDFIDE

#	Article	IF	CITATIONS
1	Understanding the corrosion inhibition of carbon steel and copper in sulphuric acid medium by amino acids using electrochemical techniques allied to molecular modelling methods. Corrosion Science, 2017, 115, 41-55.	6.6	189
2	Structural, electronic, and optical properties of ZrO2 from ab initio calculations. Journal of Applied Physics, 2006, 100, 104103.	2.5	162
3	Resveratrol prevents social deficits in animal model of autism induced by valproic acid. Neuroscience Letters, 2014, 583, 176-181.	2.1	115
4	Deformation induced martensite in an AISI 301LN stainless steel: characterization and influence on pitting corrosion resistance. Materials Research, 2007, 10, 359-366.	1.3	94
5	Graphene Nanoflakes: Thermal Stability, Infrared Signatures, and Potential Applications in the Field of Spintronics and Optical Nanodevices. Journal of Physical Chemistry C, 2010, 114, 17472-17485.	3.1	89
6	DNA-based nanobiostructured devices: The role of quasiperiodicity and correlation effects. Physics Reports, 2014, 535, 139-209.	25.6	88
7	Structural, optoelectronic, infrared and Raman spectra of orthorhombic SrSnO3 from DFT calculations. Journal of Solid State Chemistry, 2011, 184, 921-928.	2.9	85
8	Explaining statin inhibition effectiveness of HMG-CoA reductase by quantum biochemistry computations. Physical Chemistry Chemical Physics, 2012, 14, 1389-1398.	2.8	61
9	First-principles calculations of structural, electronic, and optical absorption properties of CaCO3 Vaterite. Chemical Physics Letters, 2007, 435, 59-64.	2.6	60
10	Coexistence of triclinic and monoclinic phases in WO3 ceramics. Journal of Raman Spectroscopy, 2000, 31, 451-454.	2.5	58
11	Form of the quantum kinetic-energy operator with spatially varying effective mass. Physical Review B, 1997, 55, 1326-1328.	3.2	54
12	Electronic properties of a quasi-two-dimensional electron gas in semiconductor quantum wells under intense laser fields. Physical Review B, 2004, 70, .	3.2	54
13	Möbius and twisted graphene nanoribbons: Stability, geometry, and electronic properties. Journal of Chemical Physics, 2008, 128, 164719.	3.0	54
14	Structural and optoelectronic properties, and infrared spectrum of cubic BaSnO3 from first principles calculations. Journal of Applied Physics, 2012, 112, .	2.5	54
15	Polarized Raman, <scp>FTIR,</scp> and <scp>DFT</scp> study of <scp>Na₂Ti₃O₇</scp> microcrystals. Journal of Raman Spectroscopy, 2018, 49, 538-548.	2.5	54
16	Full-relativistic calculations of the SrTiO3 carrier effective masses and complex dielectric function. Applied Physics Letters, 2003, 82, 3074-3076.	3.3	53
17	Optical absorption and DFT calculations in <mml:math xmlns:mml="http://www.w3.org/1998/Math/MathML" display="inline"> <mml:mi>L</mml:mi> -aspartic acid anhydrous crystals: Charge carrier effective masses point to semiconducting behavior. Physical Review B. 2012. 86</mml:math 	3.2	51
18	Intraband absorption and Stark effect in silicon nanocrystals. Physical Review B, 2005, 72, .	3.2	50

#	Article	IF	CITATIONS
19	Three-dimensional self-consistent simulation of the charging time response in silicon nanocrystal flash memories. Journal of Applied Physics, 2002, 92, 6182-6187.	2.5	47
20	Structural and electronic properties of SrxBa1â^'xSnO3 from first principles calculations. Journal of Solid State Chemistry, 2012, 187, 186-194.	2.9	47
21	Anhydrous crystals of DNA bases are wide gap semiconductors. Journal of Chemical Physics, 2011, 134, 175101.	3.0	45
22	Production and characterization of the cashew (Anacardium occidentale L.) peduncle bagasse ashes. Journal of Food Engineering, 2007, 79, 1432-1437.	5.2	44
23	Quantum molecular modelling of ibuprofen bound to human serum albumin. RSC Advances, 2015, 5, 49439-49450.	3.6	42
24	Interface-related exciton-energy blueshift inGaN/AlxGa1â^'xNzinc-blende and wurtzite single quantum wells. Physical Review B, 1999, 60, 5705-5713.	3.2	41
25	Slab lenses from simple anisotropic media. Physical Review B, 2005, 72, .	3.2	40
26	Elucidating the high-k insulator α-Al2O3 direct/indirect energy band gap type through density functional theory computations. Chemical Physics Letters, 2015, 637, 172-176.	2.6	40
27	Structural, electronic, and optical properties of CaCO3 aragonite. Chemical Physics Letters, 2006, 430, 293-296.	2.6	38
28	Structural, electronic and optical properties of monoclinic Na 2 Ti 3 O 7 from density functional theory calculations: A comparison with XRD and optical absorption measurements. Journal of Solid State Chemistry, 2017, 250, 68-74.	2.9	38
29	Effective masses and complex dielectric function of cubic HfO2. Applied Physics Letters, 2004, 85, 5022-5024.	3.3	37
30	Optical absorption and electronic band structure first-principles calculations of <mml:math xmlns:mml="http://www.w3.org/1998/Math/MathML" display="inline"><mml:mi>ì±</mml:mi>-glycine crystals. Physical Review B, 2008, 77, .</mml:math 	3.2	37
31	Antipsychotic Haloperidol Binding to the Human Dopamine D3 Receptor: Beyond Docking Through QM/MM Refinement Toward the Design of Improved Schizophrenia Medicines. ACS Chemical Neuroscience, 2014, 5, 1041-1054.	3.5	37
32	RA Differentiation Enhances Dopaminergic Features, Changes Redox Parameters, and Increases Dopamine Transporter Dependency in 6-Hydroxydopamine-Induced Neurotoxicity in SH-SY5Y Cells. Neurotoxicity Research, 2017, 31, 545-559.	2.7	37
33	Phase transition in WO3microcrystals obtained by sintering process. Journal of Raman Spectroscopy, 2001, 32, 695-699.	2.5	36
34	Electronic and optical properties of CaCO ₃ calcite, and excitons in Si@CaCO ₃ and CaCO ₃ @SiO ₂ core-shell quantum dots. Journal Physics D: Applied Physics, 2007, 40, 5747-5752.	2.8	36
35	Pressure effects in the Raman spectrum ofWO3microcrystals. Physical Review B, 2000, 62, 3699-3703.	3.2	35
36	Crystal structure of a lectin from Canavalia maritima (ConM) in complex with trehalose and maltose reveals relevant mutation in ConA-like lectins. Journal of Structural Biology, 2006, 154, 280-286.	2.8	34

#	Article	IF	CITATIONS
37	Acoustic phonon transmission spectra in piezoelectric AlN/GaN Fibonacci phononic crystals. European Physical Journal B, 2007, 58, 379-387.	1.5	34
38	Evidence of magnetic polaronic states inLa0.70Sr0.30Mn1â^'xFexO3manganites. Physical Review B, 2003, 67, .	3.2	33
39	Role of Cu, Ni and Co metals in the acidic and redox properties of Mo catalysts supported on Al ₂ O ₃ spheres for glycerol conversion. Catalysis Science and Technology, 2016, 6, 4986-5002.	4.1	33
40	Velocity overshoot onset in nitride semiconductors. Applied Physics Letters, 2000, 76, 1893-1895.	3.3	32
41	Quantum biochemistry study of the T3-785 tropocollagen triple-helical structure. Chemical Physics Letters, 2013, 559, 88-93.	2.6	31
42	A quantum biochemistry investigation of willardiine partial agonism in AMPA receptors. Physical Chemistry Chemical Physics, 2015, 17, 13092-13103.	2.8	31
43	DFT Calculations with van der Waals Interactions of Hydrated Calcium Carbonate Crystals CaCO ₃ A·(H ₂ 0, 6H ₂ 0): Structural, Electronic, Optical, and Vibrational Properties. Journal of Physical Chemistry A, 2016, 120, 5752-5765.	2.5	31
44	Adsorption of Ascorbic Acid on the C ₆₀ Fullerene. Journal of Physical Chemistry B, 2008, 112, 14267-14272.	2.6	30
45	An improved description of the dielectric breakdown in oxides based on a generalized Weibull distribution. Physica A: Statistical Mechanics and Its Applications, 2006, 361, 209-215.	2.6	29
46	Structural, electronic, and optical absorption properties of orthorhombic CaSnO3throughab initiocalculations. Journal of Physics Condensed Matter, 2007, 19, 106214.	1.8	29
47	Ultrafast mobility in photoinjected polar semiconductors. Physical Review B, 1989, 39, 13264-13275.	3.2	28
48	A quantum chemistry investigation of a potential inhibitory drug against the dengue virus. RSC Advances, 2016, 6, 56562-56570.	3.6	28
49	Production in Pichia pastoris, antifungal activity and crystal structure of a class I chitinase from cowpea (Vigna unguiculata): Insights into sugar binding mode and hydrolytic action. Biochimie, 2017, 135, 89-103.	2.6	28
50	<scp>l</scp> -Serine Anhydrous Crystals: Structural, Electronic, and Optical Properties by First-Principles Calculations, and Optical Absorption Measurement. Crystal Growth and Design, 2013, 13, 2793-2802.	3.0	27
51	Structural and electronic properties of CaSiO3 triclinic. Chemical Physics Letters, 2006, 427, 113-116.	2.6	26
52	Crystal structure of Dioclea rostrata lectin: Insights into understanding the pH-dependent dimer-tetramer equilibrium and the structural basis for carbohydrate recognition in Diocleinae lectins. Journal of Structural Biology, 2008, 164, 177-182.	2.8	26
53	Defects in Graphene-Based Twisted Nanoribbons: Structural, Electronic, and Optical Properties. Langmuir, 2009, 25, 4751-4759.	3.5	26
54	Coal Fly Ash Ceramics: Preparation, Characterization, and Use in the Hydrolysis of Sucrose. Scientific World Journal, The, 2014, 2014, 1-7.	2.1	26

#	Article	IF	CITATIONS
55	Carbon fiber/epoxy composites: effect of zinc sulphide coated carbon nanotube on thermal and mechanical properties. Polymer Bulletin, 2018, 75, 1619-1633.	3.3	26
56	Immobilization of urease on vapour phase stain etched porous silicon. Process Biochemistry, 2007, 42, 429-433.	3.7	25
57	Angiotensin Converting Enzyme Regulates Cell Proliferation and Migration. PLoS ONE, 2016, 11, e0165371.	2.5	25
58	A quantum biochemistry model of the interaction between the estrogen receptor and the two antagonists used in breast cancer treatment. Computational and Theoretical Chemistry, 2016, 1089, 21-27.	2.5	25
59	Quantum binding energy features of the T3-785 collagen-like triple-helical peptide. RSC Advances, 2017, 7, 2817-2828.	3.6	25
60	Nonlinear transport properties of III-nitrides in electric field. Journal of Applied Physics, 2005, 98, 043702.	2.5	24
61	Two-Level Adsorption of Ibuprofen on C ₆₀ Fullerene for Transdermal Delivery: Classical Molecular Dynamics and Density Functional Theory Computations. Journal of Physical Chemistry C, 2011, 115, 24501-24511.	3.1	24
62	Nanoencapsulation of benznidazole in calcium carbonate increases its selectivity to <i>Trypanosoma cruzi</i> . Parasitology, 2018, 145, 1191-1198.	1.5	24
63	Microstructural and electrical properties of sintered tungsten trioxide. Journal of Materials Science, 1999, 34, 1031-1035.	3.7	23
64	Antimicrobial effect of <i>Dinoponera quadriceps</i> (Hymenoptera: Formicidae) venom against <i>Staphylococcus aureus</i> strains. Journal of Applied Microbiology, 2014, 117, 390-396.	3.1	23
65	Carbon steel corrosion inhibition in acid medium by imidazole-based molecules: Experimental and molecular modelling approaches. Journal of Molecular Liquids, 2021, 326, 115330.	4.9	23
66	Hole mobility in zincblende c–GaN. Journal of Applied Physics, 2004, 95, 4914-4917.	2.5	22
67	<mml:math <br="" altimg="si24.gif" display="inline" xmlns:mml="http://www.w3.org/1998/Math/MathML">overflow="scroll"><mml:mrow><mml:msub><mml:mrow><mml:mtext>CdXO</mml:mtext></mml:mrow><mu (X = C, Si, Ge, Sn, Pb) electronic band structures. Chemical Physics Letters, 2009, 480, 273-277.</mu </mml:msub></mml:mrow></mml:math>	ml:mໝໜ່><ເ	mm ៤ខ ាព>3
68	Triclinic CdSiO ₃ structural, electronic, and optical properties from first principles calculations. Journal Physics D: Applied Physics, 2009, 42, 155406.	2.8	22
69	Assessing the Role of Water on the Electronic Structure and Vibrational Spectra of Monohydrated <scp>l</scp> -Aspartic Acid Crystals. Crystal Growth and Design, 2013, 13, 4844-4851.	3.0	22
70	Vibrational Spectroscopy and Phonon-Related Properties of the <scp>l</scp> -Aspartic Acid Anhydrous Monoclinic Crystal. Journal of Physical Chemistry A, 2015, 119, 11791-11803.	2.5	22
71	Simple synthesis of Al2O3 sphere composite from hybrid process with improved thermal stability for catalytic applications. Materials Chemistry and Physics, 2015, 160, 119-130.	4.0	22
72	Purification, Biochemical Characterization, and Amino Acid Sequence of a Novel Type of Lectin from Aplysia dactylomela Eggs with Antibacterial/Antibiofilm Potential. Marine Biotechnology, 2017, 19, 49-64.	2.4	22

#	Article	IF	CITATIONS
73	Hot Electron Dynamics in Zincblende and Wurtzite GaN. Physica Status Solidi (B): Basic Research, 1999, 216, 35-39.	1.5	21
74	Confinement of two-dimensional excitons in a nonhomogeneous magnetic field. Physical Review B, 2000, 61, 2895-2903.	3.2	21
75	Molecular Signature in the Photoluminescence of α-Glycine, L-Alanine and L-Asparagine Crystals: Detection, ab initio Calculations, and Bio-sensor Applications. AIP Conference Proceedings, 2005, , .	0.4	21
76	Trypanocidal activity of mastoparan from Polybia paulista wasp venom by interaction with TcGAPDH. Toxicon, 2017, 137, 168-172.	1.6	21
77	Velocity overshoot in zincblende and wurtzite GaN. Solid State Communications, 1999, 110, 469-472.	1.9	20
78	Urbach's tail in III-nitrides under an electric field. Journal of Applied Physics, 2001, 90, 1879-1882.	2.5	20
79	Hot-phonon bottleneck in the photoinjected plasma in GaN. Applied Physics Letters, 2003, 82, 2455-2457.	3.3	20
80	Ab initio structural, electronic and optical properties of orthorhombic. Journal of Solid State Chemistry, 2007, 180, 974-980.	2.9	20
81	Structural, electronic and optical properties of ilmenite and perovskite CdSnO ₃ from DFT calculations. Journal of Physics Condensed Matter, 2010, 22, 435801.	1.8	20
82	Inactivation of Ovine Cyclooxygenase-1 by Bromoaspirin and Aspirin: A Quantum Chemistry Description. Journal of Physical Chemistry B, 2012, 116, 3270-3279.	2.6	20
83	The vibrational properties of the bee-killer imidacloprid insecticide: A molecular description. Spectrochimica Acta - Part A: Molecular and Biomolecular Spectroscopy, 2017, 185, 245-255.	3.9	20
84	Energetic description of cilengitide bound to integrin. New Journal of Chemistry, 2017, 41, 11405-11412.	2.8	20
85	Effects of crystallographic orientations on the charging time in silicon nanocrystal flash memories. Applied Physics Letters, 2003, 82, 2685-2687.	3.3	19
86	Structural and optical properties of CaO. Microelectronics Journal, 2005, 36, 1058-1061.	2.0	19
87	Nonlinear transport properties of doped III-N and GaAs polar semiconductors: A comparison. Journal of Applied Physics, 2005, 98, 043703.	2.5	19
88	Monoclinic and orthorhombic cysteine crystals are small gap insulators. Chemical Physics Letters, 2011, 512, 208-210.	2.6	19
89	Ribosomal RNA–Aminoglycoside Hygromycin B Interaction Energy Calculation within a Density Functional Theory Framework. Journal of Physical Chemistry B, 2019, 123, 6421-6429.	2.6	19
90	The urokinase plasminogen activator binding to its receptor: a quantum biochemistry description within an in/homogeneous dielectric function framework with application to uPA–uPAR peptide inhibitors. Physical Chemistry Chemical Physics, 2020, 22, 3570-3583.	2.8	19

#	Article	IF	CITATIONS
91	Band Structure Derived Properties of HfO2 from First Principles Calculations. AIP Conference Proceedings, 2005, , .	0.4	18
92	Hole-versus electron-based operations in SiGe nanocrystal nonvolatile memories. Applied Physics Letters, 2007, 90, 223504.	3.3	18
93	The quantum biophysics of the isoniazid adduct NADH binding to its InhA reductase target. New Journal of Chemistry, 2014, 38, 2946.	2.8	18
94	A comparative density functional theory study of electronic structure and optical properties of -aminobutyric acid and its cocrystals with oxalic and benzoic acid. Chemical Physics Letters, 2013, 587, 20-24.	2.6	17
95	Controlled Release of Nor-β-Iapachone by PLGA Microparticles: A Strategy for Improving Cytotoxicity against Prostate Cancer Cells. Molecules, 2016, 21, 873.	3.8	17
96	Anhydrous proline crystals: Structural optimization, optoelectronic properties, effective masses and Frenkel exciton energy. Journal of Physics and Chemistry of Solids, 2018, 121, 36-48.	4.0	17
97	Electron mobility in nitride materials. Brazilian Journal of Physics, 2002, 32, 439-441.	1.4	17
98	Computational investigation of the α ₂ β ₁ integrin–collagen triple helix complex interaction. New Journal of Chemistry, 2018, 42, 17115-17125.	2.8	16
99	L-asparagine crystals with wide gap semiconductor features: Optical absorption measurements and density functional theory computations. Journal of Chemical Physics, 2014, 140, 124511.	3.0	15
100	Structural basis of ConM binding with resveratrol, an anti-inflammatory and antioxidant polyphenol. International Journal of Biological Macromolecules, 2015, 72, 1136-1142.	7.5	15
101	Quantum Biochemistry Description of the Human Dopamine D3 Receptor in Complex with the Selective Antagonist Eticlopride. Journal of Proteomics and Bioinformatics, 2012, 05, .	0.4	15
102	High-magnetic-field effects on the terahertz mobility of hot electrons inn-type InSb. Physical Review B, 1998, 57, 11872-11874.	3.2	14
103	Smooth interface effects on the Raman scattering in zinc-blende AlN/GaN superlattices. Physical Review B, 2000, 61, 13060-13063.	3.2	14
104	Transient transport in III-nitrides: interplay of momentum and energy relaxation times. Journal of Physics Condensed Matter, 2007, 19, 346214.	1.8	14
105	Identification of lamivudine conformers by Raman scattering measurements and quantum chemical calculations. Journal of Pharmaceutical and Biomedical Analysis, 2007, 43, 1885-1889.	2.8	14
106	A renormalization approach to describe charge transport in quasiperiodic dangling backbone ladder (DBL)-DNA molecules. Physics Letters, Section A: General, Atomic and Solid State Physics, 2011, 375, 3993-3996.	2.1	14
107	Phosphate group vibrational signatures of the osteoporosis drug alendronate. Journal of Raman Spectroscopy, 2014, 45, 801-806.	2.5	14
108	Two Binding Geometries for Risperidone in Dopamine D3 Receptors: Insights on the Fast-Off Mechanism through Docking, Quantum Biochemistry, and Molecular Dynamics Simulations. ACS Chemical Neuroscience, 2016, 7, 1331-1347.	3.5	14

#	Article	IF	CITATIONS
109	Rose Bengal incorporated to α-cyclodextrin microparticles for photodynamic therapy against the cariogenic microorganism Streptococcus mutans. Photodiagnosis and Photodynamic Therapy, 2019, 25, 111-118.	2.6	14
110	Highâ€field transport transient of minority carriers inpâ€GaAs. Applied Physics Letters, 1991, 59, 558-560.	3.3	13
111	Exciton confinement in InGaN/GaN cylindrical quantum wires. Brazilian Journal of Physics, 2004, 34, 702-704.	1.4	13
112	Crystallization and preliminary X-ray diffraction analysis of the lectin fromCanavalia gladiataseeds. Acta Crystallographica Section D: Biological Crystallography, 2004, 60, 1493-1495.	2.5	13
113	Correlation betweenEnterococcus faecalisBiofilms Development Stage and Quantitative Surface Roughness Using Atomic Force Microscopy. Microscopy and Microanalysis, 2008, 14, 150-158.	0.4	13
114	Four-level levodopa adsorption on C60 fullerene for transdermal and oral administration: a computational study. RSC Advances, 2012, 2, 8306.	3.6	13
115	The DNA electronic specific heat at low temperature: The role of aperiodicity. Physics Letters, Section A: General, Atomic and Solid State Physics, 2012, 376, 2413-2417.	2.1	13
116	Direct electrochemical analysis of dexamethasone endocrine disruptor in raw natural waters. Journal of the Brazilian Chemical Society, 2012, 23, 110-119.	0.6	13
117	Immobilized invertase studies on glass–ceramic support from coal fly ashes. Chemical Engineering Journal, 2013, 214, 91-96.	12.7	13
118	Structural, Electronic, and Optical Properties of Bulk Boric Acid <i>2A</i> and <i>3T</i> Polymorphs: Experiment and Density Functional Theory Calculations. Crystal Growth and Design, 2016, 16, 6631-6640.	3.0	13
119	Improved description of the structural and optoelectronic properties of DNA/RNA nucleobase anhydrous crystals: Experiment and dispersion-corrected density functional theory calculations. Physical Review B, 2017, 96, .	3.2	13
120	Structural and Optoelectronic Properties of the α-, β-, and γ-Glycine Polymorphs and the Glycine Dihydrate Crystal: A DFT Study. Crystal Growth and Design, 2019, 19, 5204-5217.	3.0	13
121	Resonant peaks in the transmission coefficient of compositionally nonabrupt GaAs/AlxGa1â°'xAs heterojunctions. Superlattices and Microstructures, 1992, 11, 17-22.	3.1	12
122	Fine structure of excitons in a quantum well in the presence of a nonhomogeneous magnetic field. Physical Review B, 2000, 62, 7316-7324.	3.2	12
123	Theoretical investigation of excitons in type-I and type-IISiâ^•Si1â^'xGexquantum wires. Physical Review B, 2006, 74, .	3.2	12
124	CaO first-principles electronic properties and MOS device simulation. Journal Physics D: Applied Physics, 2007, 40, 1655-1658.	2.8	12
125	The new flow system approach in packed bed reactor applicable for immobilized enzyme. Journal of Molecular Catalysis B: Enzymatic, 2012, 79, 1-7.	1.8	12
126	An ab initio explanation of the activation and antagonism strength of an AMPA-sensitive glutamate receptor. RSC Advances, 2013, 3, 14988.	3.6	12

#	Article	IF	CITATIONS
127	Cubic superparamagnetic nanoparticles of NiFe2O4 via fast microwave heating. Journal of Nanoparticle Research, 2014, 16, 1.	1.9	12
128	Computational electronic structure of the bee killer insecticide imidacloprid. New Journal of Chemistry, 2016, 40, 10353-10362.	2.8	12
129	Cloning of cDNA sequences encoding cowpea (Vigna unguiculata) vicilins: Computational simulations suggest a binding mode of cowpea vicilins to chitin oligomers. International Journal of Biological Macromolecules, 2018, 117, 565-573.	7.5	12
130	Intraband absorption in silicon nanocrystals: The combined effect of shape and crystal orientation. Applied Physics Letters, 2005, 87, 031913.	3.3	11
131	Conductance of single microRNAs chains related to the autism spectrum disorder. Europhysics Letters, 2014, 107, 68006.	2.0	11
132	Modeling of laccase inhibition by formetanate pesticide using theoretical approaches. Bioelectrochemistry, 2016, 108, 46-53.	4.6	11
133	Localization and fractal spectra of optical phonon modes in quasiperiodic structures. Physica A: Statistical Mechanics and Its Applications, 2005, 349, 259-270.	2.6	10
134	First-principles calculations of structural, electronic and optical properties of orthorhombic CaPbO ₃ . Journal Physics D: Applied Physics, 2008, 41, 065405.	2.8	10
135	Charge transport in fibrous/not fibrous α3-helical and (5Q,7Q)α3 variant peptides. Applied Physics Letters, 2011, 98, .	3.3	10
136	Sensitive voltammetric responses and mechanistic insights into the determination of residue levels of endosulfan in fresh foodstuffs and raw natural waters. Microchemical Journal, 2013, 110, 40-47.	4.5	10
137	Dimethomorph electrooxidation: Analytical determination in grape-derived samples and mechanistic aspects. Electrochimica Acta, 2013, 107, 350-357.	5.2	10
138	Optical Absorption of the Antitrypanocidal Drug Benznidazole inWater. Molecules, 2014, 19, 4145-4156.	3.8	10
139	Vibrational Properties of Bulk Boric Acid2Aand3TPolymorphs and Their Two-Dimensional Layers: Measurements and Density Functional Theory Calculations. Journal of Physical Chemistry A, 2018, 122, 1312-1325.	2.5	10
140	High magnetic field effects on the ultrafast transport transient of hot electrons in InSb. Applied Physics Letters, 1997, 70, 1879-1881.	3.3	9
141	Ultrafast electron drift velocity overshoot in 3C–SiC. Solid State Communications, 2000, 113, 539-542.	1.9	9
142	Effect of ageing on x-ray induced dopant passivation in MOS capacitors. Semiconductor Science and Technology, 2000, 15, 794-798.	2.0	9
143	A Raman scattering-based method to probe the carrier drift velocity in semiconductors: Application to gallium nitride. Applied Physics Letters, 2004, 85, 4055-4057.	3.3	9
144	Electronic transport in methylated fragments of DNA. Applied Physics Letters, 2015, 107, 203701.	3.3	9

#	Article	IF	CITATIONS
145	First-generation antipsychotic haloperidol: optical absorption measurement and structural, electronic, and optical properties of its anhydrous monoclinic crystal by first-principle approaches. New Journal of Chemistry, 2018, 42, 13629-13640.	2.8	9
146	Quantum biochemistry in cancer immunotherapy: New insights about CTLA-4/ipilimumab and design of ipilimumab-derived peptides with high potential in cancer treatment. Molecular Immunology, 2020, 127, 203-211.	2.2	9
147	ACE2-derived peptides interact with the RBD domain of SARS-CoV-2 spike glycoprotein, disrupting the interaction with the human ACE2 receptor. Journal of Biomolecular Structure and Dynamics, 2022, 40, 5493-5506.	3.5	9
148	Transmission coefficient of electrons through a single graded barrier. Physical Review B, 1993, 48, 8446-8449.	3.2	8
149	Time evolution of SiO2/Si interface defects and dopant passivation in MOS capacitors. Microelectronic Engineering, 2000, 51-52, 567-574.	2.4	8
150	Strong interface localization of phonons in nonabrupt InN/GaN superlattices. Physical Review B, 2001, 64, .	3.2	8
151	Interface-related effects on confined excitons in GaAs/AlxGa1â^'xAs single quantum wells. Applied Surface Science, 2002, 190, 191-194.	6.1	8
152	Mobility in n-doped wurtzite III-Nitrides. Materials Research, 2003, 6, 01-04.	1.3	8
153	Two different incorporation sites of manganese in single-crystalline monohydratedL-asparagine studied by electron paramagnetic resonance. Physical Review B, 2007, 75, .	3.2	8
154	C ₆₀ -derived nanobaskets: stability, vibrational signatures, and molecular trapping. Nanotechnology, 2009, 20, 395701.	2.6	8
155	Performance of invertase immobilized on glass–ceramic supports in batch bioreactor. Chemical Engineering Journal, 2012, 187, 341-350.	12.7	8
156	Electrochemical and Monte Carlo studies of self-assembled trans-[Fe(cyclam)(NCS)2]+ complex ion on gold surface as electrochemical sensor for nitric oxide. Electrochimica Acta, 2013, 91, 1-10.	5.2	8
157	An improved quantum biochemistry description of the glutamate–GluA2 receptor binding within an inhomogeneous dielectric function framework. New Journal of Chemistry, 2017, 41, 6167-6179.	2.8	8
158	CO2 role on the glycerol conversion over catalyst containing CaO-SiO2 doped with Ag and Pt. Catalysis Today, 2020, 344, 199-211.	4.4	8
159	Quantum biochemistry, molecular docking, and dynamics simulation revealed synthetic peptides induced conformational changes affecting the topology of the catalytic site of SARS-CoV-2 main protease. Journal of Biomolecular Structure and Dynamics, 2022, 40, 8925-8937.	3.5	8
160	Optical properties of ellipsoidal CdSe quantum dots. Brazilian Journal of Physics, 2006, 36, 438-439.	1.4	8
161	Electron transmission through a single nonabrupt GaAs/AlxGa1â^'xAs barrier subjected to an electric field. Physical Review B, 1995, 52, 5777-5780.	3.2	7
162	Emission spectrum in driven two-level systems. Physical Review A, 1998, 58, 1531-1536.	2.5	7

#	Article	IF	CITATIONS
163	Sign inversion of the Stark shift in single non-abrupt GaAs/AlxGa1-xAs quantum wells. Journal of Physics Condensed Matter, 1999, 11, 5593-5602.	1.8	7
164	Band structure of a cylindrical GaAs/AlxGa1â^'xAs superwire. Superlattices and Microstructures, 1999, 25, 221-225.	3.1	7
165	Band structure effects on the transient electron transport in wurtzite InN. Journal of Crystal Growth, 2002, 246, 320-324.	1.5	7
166	Optical properties of zincblende GaN/BN cylindrical nanowires. Applied Surface Science, 2004, 234, 50-53.	6.1	7
167	Effects of interfacial profiles on quantum levels in InxGa1â^'xAs/GaAs graded spherical quantum dots. Applied Surface Science, 2004, 237, 266-269.	6.1	7
168	Statistical analysis of topographic images of nanoporous silicon and model surfaces. Microelectronics Journal, 2005, 36, 1011-1015.	2.0	7
169	Energy levels in Si and SrTiO3-based quantum wells with charge image effects. Brazilian Journal of Physics, 2006, 36, 347-349.	1.4	7
170	Structural, electronic and optical properties of orthorhombic <mml:math xmlns:mml="http://www.w3.org/1998/Math/MathML" altimg="si0047.gif" overflow="scroll"><mml:msub><mml:mrow><mml:mi>CdGeO</mml:mi></mml:mrow><mml:mn> from first principles calculations. Journal of Solid State Chemistry, 2010, 183, 437-443.</mml:mn></mml:msub></mml:math 	3 <td>n > 7/mml:mro</td>	n > 7/mml:mro
171	Exploiting the Reduction of Haloperidol: Electrochemical and Computational Studies Using Silver Amalgam and HMDE Electrodes. Electrochimica Acta, 2014, 137, 564-574.	5.2	7
172	Explaining RANKL inhibition by OPG through quantum biochemistry computations and insights into peptide-design for the treatment of osteoporosis. RSC Advances, 2016, 6, 84926-84942.	3.6	7
173	Gallic acid leads to cell death of <i>Candida albicans</i> by the apoptosis mechanism. Future Microbiology, 2022, 17, 599-606.	2.0	7
174	Strong exciton energy blue shift in graded wurtzite and zincblende GaN/Al0.2Ga0.8N single quantum wells. Journal of Crystal Growth, 2002, 246, 341-346.	1.5	6
175	Strong graded interface related exciton energy blueshift in InxGa1â^'xN/GaN quantum dots. Physica E: Low-Dimensional Systems and Nanostructures, 2003, 17, 22-23.	2.7	6
176	Large image potential effects in Siâ^•SrTiO3 and Siâ^•HfO2 two-dimensional quantum well structures. Applied Physics Letters, 2006, 88, 242114.	3.3	6
177	AFM and hydrodynamic electrochemical characterization of the self-assembled 1,4-dithiane on gold surface. Journal of Electroanalytical Chemistry, 2007, 603, 21-26.	3.8	6
178	The influence of 4-mercaptopyridine layer instability on rapid electron transfer reaction. Journal of Electroanalytical Chemistry, 2008, 619-620, 26-30.	3.8	6
179	Thermal effect on the dielectric function and small polaron hopping conduction in organic molecular crystals. Physics Letters, Section A: General, Atomic and Solid State Physics, 2008, 372, 3725-3728.	2.1	6
180	cDNA cloning, molecular modeling and docking calculations of L -type lectins from Swartzia simplex var. grandiflora (Leguminosae, Papilionoideae), a member of the tribe Swartzieae. Phytochemistry, 2017, 139, 60-71.	2.9	6

#	Article	IF	CITATIONS
181	Encapsulation of nor-β-lapachone into poly(<scp>d</scp> , <scp>l</scp>)-lactide-co-glycolide (PLGA) microcapsules: full characterization, computational details and cytotoxic activity against human cancer cell lines. MedChemComm, 2017, 8, 1993-2002.	3.4	6
182	Copper promoter effect on acid–base and redox sites of Fe/Al ₂ O ₃ catalysts and their role in ethanol–acetone mixture conversion. Catalysis Science and Technology, 2018, 8, 443-458.	4.1	6
183	Computational approach, scanning electron and fluorescence microscopies revealed insights into the action mechanisms of anticandidal peptide Mo-CBP3-PepIII. Life Sciences, 2021, 281, 119775.	4.3	6
184	Antitumor Potential of the Isoflavonoids (+)- and (â^')-2,3,9-Trimethoxypterocarpan: Mechanism-of-Action Studies. ACS Medicinal Chemistry Letters, 2020, 11, 1274-1280.	2.8	6
185	Structured ultrafast mobility in highly photoexcited semiconductors. Solid State Communications, 1988, 66, 683-687.	1.9	5
186	Transmission in compositionally nonabrupt GaAs/AlxGa1-xAs heterojunctions: beyond the constant interfacial effective-mass approximation. Superlattices and Microstructures, 1995, 17, 123-128.	3.1	5
187	Electrostatic surface shape resonances of a finite number of ridges. European Physical Journal B, 1998, 3, 119-123.	1.5	5
188	Strong interface effects in graded SiO2/Si/SiO2 quantum wells. Journal of Applied Physics, 1998, 84, 5369-5371.	2.5	5
189	Structured Ultrafast Carrier Drift Velocity in Photoexcited Zincblende GaN. Materials Science Forum, 2000, 338-342, 1579-1582.	0.3	5
190	Strong graded interface related piezoelectric polarization weakening effects on exciton confinement in single InxGa1â^^xN/GaN quantum wells. Physica E: Low-Dimensional Systems and Nanostructures, 2002, 13, 1106-1110.	2.7	5
191	A percolation based dielectric breakdown model with randomic changes in the dielectric constant. Physica A: Statistical Mechanics and Its Applications, 2002, 305, 351-359.	2.6	5
192	Interfacial fluctuations effects on confined excitons in single GaAs/AlxGa1â^'xAs quantum wells. Surface Science, 2003, 532-535, 774-779.	1.9	5
193	Inhomogeneous broadening arising from interface fluctuations in strained InxGa1â^'xAs/GaAs and (InuGa1â^'uAs)v(InP)1â^'v/InP quantum wells. Applied Surface Science, 2004, 234, 38-44.	6.1	5
194	Acoustic phonon dynamics in strained cubic and hexagonal GaN/Al2O3 superlattices. European Physical Journal B, 2006, 51, 583-591.	1.5	5
195	Influence of graded interfaces on the exciton energy of type-I and type-II Si/Si1-x Gex quantum wires. Journal of Materials Science, 2007, 42, 2314-2317.	3.7	5
196	Interaction energy profile for diphenyl diselenide in complex with δ-aminolevulinic acid dehydratase enzyme using quantum calculations and a molecular fragmentation method. Computational Toxicology, 2018, 7, 9-19.	3.3	5
197	Structural, electronic, and optical properties of inhomogeneous Ca1â^x Mg x O alloys. Journal of Applied Physics, 2019, 125, 155102.	2.5	5
198	mTOR–mLST8 interaction: hot spot identification through quantum biochemistry calculations. New Journal of Chemistry, 2020, 44, 20982-20992.	2.8	5

#	Article	IF	CITATIONS
199	Transmission in symmetrical GaAs/AlxGa1-xAs double-barriers with compositionally nonabrupt interfaces. Superlattices and Microstructures, 1994, 15, 203.	3.1	4
200	Energy levels of single nonabrupt GaAs/AlxGa1-xAs quantum wells. Superlattices and Microstructures, 1995, 17, 397.	3.1	4
201	Energy level splitting in doped nonabrupt double quantum well. Solid State Communications, 1998, 106, 559-562.	1.9	4
202	Graded interface effects on the carriers confinement in single GaN/AlxGa1â^'xN wurtzite quantum wells. Solid State Communications, 1999, 110, 587-592.	1.9	4
203	Dynamics of SiO2/SiOx/Si multilayer growth and interfacial effects on silicon quantum well confinement properties. Materials Science and Engineering B: Solid-State Materials for Advanced Technology, 2000, 74, 188-192.	3.5	4
204	Strong exciton energy blue shift in annealed Si/SiO2 single quantum wells. Applied Surface Science, 2000, 166, 469-474.	6.1	4
205	Strong interface-induced changes on the numerical calculated Raman scattering in Si/3C–SiC superlattices. Applied Physics Letters, 2000, 77, 4316-4318.	3.3	4
206	Theory of exciton–polariton in GaN thin films. Solid State Communications, 2002, 124, 109-112.	1.9	4
207	Optical phonon modes in graded III–V nitride quantum wells. Solid State Communications, 2005, 135, 308-313.	1.9	4
208	Dielectric mismatch effects on the electronic and optical properties of GaNâ^+HfO2 quantum wells. Applied Physics Letters, 2005, 87, 171904.	3.3	4
209	Electronic and optical properties of CaCO3 porous nanoparticles. Journal of Applied Physics, 2006, 100, 034314.	2.5	4
210	Carbon-based nanorings sliding along inner coaxial nanotubes: Möbius topology effects in damping gigahertz oscillations. Journal of Applied Physics, 2014, 116, 124311.	2.5	4
211	Changing the gap type of solid state boric acid by heating: a dispersion-corrected density functional study of l±-, l²-, and l³-metaboric acid polymorphs. New Journal of Chemistry, 2017, 41, 15533-15544.	2.8	4
212	Vibrational Modes and Phonon and Thermodynamic Properties of the Metaboric Acid Polymorphs α-, β-, and γ-(BOH) ₃ O ₃ within a Density Functional Theory Framework. Journal of Physical Chemistry A, 2018, 122, 7628-7645.	2.5	4
213	Explaining urokinase type plasminogen activator inhibition by amino-5-hydroxybenzimidazole and two naphthamidine-based compounds through quantum biochemistry. Physical Chemistry Chemical Physics, 2018, 20, 22818-22830.	2.8	4
214	Solid state properties of hydroxyurea: Optical absorption measurement and DFT calculations. Journal of Applied Physics, 2019, 125, 134901.	2.5	4
215	Novel Si-C compounds with semiconducting and metallic properties: A DFT study. Computational Materials Science, 2020, 183, 109800.	3.0	4
216	Betaine-loaded CaCO3 microparticles improve survival of vitrified feline preantral follicles through higher mitochondrial activity and decreased reactive oxygen species. Reproduction, Fertility and Development, 2020, 32, 531.	0.4	4

#	Article	IF	CITATIONS
217	New ethionamide boosters and EthR2: structural and energetic analysis. Physical Chemistry Chemical Physics, 2021, 23, 23233-23241.	2.8	4
218	Nonlinear transport in far-from-equilibrium semiconductors. Nuovo Cimento Della Societa Italiana Di Fisica D - Condensed Matter, Atomic, Molecular and Chemical Physics, Biophysics, 1990, 12, 1387-1404.	0.4	3
219	The Thermalization Process of Photoexcited Electrons and Holes in the Second Kinetic Stage of Relaxation. Physica Status Solidi (B): Basic Research, 1993, 180, 213-222.	1.5	3
220	Doping profile effects on modulation-doped single nonabrupt GaAs/AlxGa1â^'xAs quantum wells. Superlattices and Microstructures, 1999, 25, 307-311.	3.1	3
221	Confined electron and shallow donor states in graded GaAs/Al Ga As spherical quantum dots. European Physical Journal B, 2000, 14, 337-348.	1.5	3
222	Exciton energy broadening due to interface fluctuations in ZnSe/ZnSxSe1â^'x strained quantum wells. Applied Surface Science, 2002, 190, 247-251.	6.1	3
223	The influence of graded interfaces in the electronic spectrum of nanometer silicon dots. Applied Surface Science, 2002, 190, 166-170.	6.1	3
224	Band structure anisotropy effects on the hole transport transient in 4H–SiC. Microelectronics Journal, 2003, 34, 717-719.	2.0	3
225	Exciton-based photoluminescence broadening in graded ZnSe/ZnSxSe1â^'x strained quantum wells. Physica E: Low-Dimensional Systems and Nanostructures, 2003, 17, 225-226.	2.7	3
226	Effect of residual acceptors on electron mobility in single asymmetric quantum wells. Physica E: Low-Dimensional Systems and Nanostructures, 2003, 17, 322-323.	2.7	3
227	Interface properties in ZnSe/ZnS based strained superlattices and quantum wells. Applied Surface Science, 2004, 237, 261-265.	6.1	3
228	Interface effects in modulation-doped GaAs/AlGaAs single quantum wells and superlattices. Microelectronics Journal, 2005, 36, 359-361.	2.0	3
229	Quantum mechanicalab initiocalculations of the Raman scattering from psoralens. Journal of Physics Condensed Matter, 2006, 18, 8325-8336.	1.8	3
230	Density functional theory study of the electronic properties of naphthofuranquinone compounds with antitrypanocidal activity. International Journal of Quantum Chemistry, 2011, 111, 1270-1279.	2.0	3
231	Electronic specific heat of an α3-helical polypeptide and its biochemical variants. Chemical Physics Letters, 2012, 542, 123-127.	2.6	3
232	<i>In silico</i> approach of modified melanoma peptides and their immunotherapeutic potential. Physical Chemistry Chemical Physics, 2021, 23, 2836-2845.	2.8	3
233	High temperature behavior of subpicosecond electron transport transient in 3C- and 6H-SiC. Brazilian Journal of Physics, 1999, 29, 785-789.	1.4	3
234	Optical absorption measurements and optoelectronic DFT calculations for ethanol solvated quercetin and anhydrous/hydrated quercetin crystals. Journal of Solid State Chemistry, 2022, 312, 123242.	2.9	3

#	Article	IF	CITATIONS
235	Transport in photoexcited hot carriers systems. Solid-State Electronics, 1988, 31, 497-499.	1.4	2
236	The time response of photoexcited carriers to strong high-frequency and constant electric fields. Solid State Communications, 1990, 76, 631-634.	1.9	2
237	On the transmission coefficient of graded composition GaAs/AlxGa1â^'xAs heterojunctions under an electric field. Journal of Applied Physics, 1992, 71, 4076-4078.	2.5	2
238	Interface effects in the high electric field resonances of single AlxGa1-xAs non-abrupt barriers in GaAs. Superlattices and Microstructures, 1995, 17, 235-239.	3.1	2
239	Interface effects on the resonant tunnelling in GaAs/Al Ga1â^'As double-quantum-well triple-barriers. Microelectronic Engineering, 1998, 43-44, 191-195.	2.4	2
240	Dissipative quantum tunneling of two-level systems driven by dc-ac fields. Physical Review E, 1998, 58, 2632-2635.	2.1	2
241	Electric field effects on the confinement properties of GaN/Al x Ga1-xN zincblende and wurtzite nonabrupt quantum wells. Brazilian Journal of Physics, 1999, 29, 670-674.	1.4	2
242	Blue and red Stark shifts in single Si/SiO2quantum wells. Superlattices and Microstructures, 1999, 25, 377-381.	3.1	2
243	Scaling properties of the electronic structure of quasiperiodic GaAs/AlxGa1â^'xAs superwires and superdots. Physica B: Condensed Matter, 2001, 305, 38-47.	2.7	2
244	Exciton trapping in a hybrid ferromagnetic/semiconductor magnetic antidot. Journal of Magnetism and Magnetic Materials, 2001, 226-230, 2038-2039.	2.3	2
245	Interface effects in the Raman scattering of InN/AIN superlattices. Physical Review B, 2002, 66, .	3.2	2
246	Terahertz complex mobility of hot electrons in 3C– and 6H–SiC at high temperature. Journal of Applied Physics, 2002, 91, 5208-5212.	2.5	2
247	The Role of Interfaced Modes in the Raman Spectra of AlN/InN Superlattices. Physica Status Solidi A, 2002, 194, 506-509.	1.7	2
248	Magnetic confinement of electrons into quantum wires and dots on a liquid helium surface. Physica E: Low-Dimensional Systems and Nanostructures, 2002, 12, 946-949.	2.7	2
249	The role of multiple damaged layers at the Si/SiO2 interface on the dielectric breakdown of MOS capacitors. Applied Surface Science, 2002, 190, 35-38.	6.1	2
250	The impact of high-k dielectrics in nanocrystal flash memories. , 2005, 5732, 547.		2
251	Gate inversion effect in Si1â^'xGexâ^•HfO2â^•Si metal-oxide-semiconductor devices. Applied Physics Letters, 2005, 86, 243507.	3.3	2
252	Crystal structure and specific location of a germin-like protein with proteolytic activity from Thevetia peruviana. Plant Science, 2020, 298, 110590.	3.6	2

#	Article	IF	CITATIONS
253	Insulin degludec and glutamine dipeptide modify glucose homeostasis and liver metabolism in diabetic mice undergoing insulin-induced hypoglycemia. Journal of Applied Biomedicine, 2021, 19, 210-219.	1.7	2
254	On the coherent tunneling current in semiconductor heterostructures. Solid State Communications, 1992, 82, 363-365.	1.9	1
255	High field transient of photoexcited GaAs electrons and holes with acoustic and to-phonon momentum scattering. Solid State Communications, 1992, 84, 927-930.	1.9	1
256	Accumulation layer and interface effects in doped nonabrupt GaAs/AlxGa1-xAs heterojunctions. Superlattices and Microstructures, 1995, 17, 351.	3.1	1
257	The influence of interfacial growth patterns on the transmission properties of carriers through nonabrupt GaAs/AlxGa1-xAs single barriers. Superlattices and Microstructures, 1995, 17, 411.	3.1	1
258	The influence of growth patterns on the transmission properties of nonabrupt GaAs/AlxGa1â^'xAs heterojunctions. Superlattices and Microstructures, 1996, 20, 155-161.	3.1	1
259	Accumulation layer and interface effects in doped nonabrupt GaAs/AlxGa1â^'xAs single quantum wells. Superlattices and Microstructures, 1998, 23, 1015-1018.	3.1	1
260	Energy States in Graded Cylindrical GaAs/AlxGa1?xAs Quantum Wires. Physica Status Solidi (B): Basic Research, 1998, 210, 75-80.	1.5	1
261	Effects of interfacial charges on semiconductor films. Physical Review B, 1998, 57, 12275-12280.	3.2	1
262	Energy level broadening control in quantum dots by interfacial doping. Solid State Communications, 1999, 113, 115-119.	1.9	1
263	High-Frequency Electron Mobility in GaN. Physica Status Solidi (B): Basic Research, 1999, 216, 737-742.	1.5	1
264	Recombination energy changes due to shell-like defects in Si/SiO2 quantum dots. Physica E: Low-Dimensional Systems and Nanostructures, 2003, 17, 73-76.	2.7	1
265	Optical gain in non-abrupt GaAs/AlxGa1â^'x quantum well lasers. Physica E: Low-Dimensional Systems and Nanostructures, 2003, 17, 600-601.	2.7	1
266	A multi-defect initialization-based percolation model: a successful scheme to explain dielectric breakdown in MOS devices. Physica E: Low-Dimensional Systems and Nanostructures, 2003, 17, 645-647.	2.7	1
267	Transport Transient of Electrons in Wurtzite InN: The Effect of the Band Structure Anisotropy. Physica Status Solidi C: Current Topics in Solid State Physics, 2003, 0, 368-372.	0.8	1
268	Confined excitons in Si/SrTiO3 quantum wells. Microelectronics Journal, 2003, 34, 507-509.	2.0	1
269	Electronic spectra of GaAs/GaxAl1â^'xAs superlattice with impurities arranged according to a Fibonacci sequence. Applied Surface Science, 2004, 234, 33-37.	6.1	1
270	Γ́(r) type model for interface defects in Si/SiO2 nanocrystals. Applied Surface Science, 2004, 234, 218-221.	6.1	1

#	Article	IF	CITATIONS
271	Sporopollenin Nanostructure of Ilex paraguariensis A.St.Hil Pollen Grains. Microscopy and Microanalysis, 2005, 11, 78-81.	0.4	1
272	Interface optical phonon localization in graded GaN thin films. Physics Letters, Section A: General, Atomic and Solid State Physics, 2005, 336, 259-263.	2.1	1
273	Lifetime of quasi-bound states in open semiconductor quantum structures. Physica Status Solidi C: Current Topics in Solid State Physics, 2005, 2, 3031-3034.	0.8	1
274	Carrier confinement in AlGaN non-abrupt heterostructured nanowires. Physica Status Solidi C: Current Topics in Solid State Physics, 2005, 2, 2365-2368.	0.8	1
275	Towards Using Multiferroism in Optoelectronics and Spintronics: Tunneling, Confinement and Optical Properties of Si/BiMnO3 Systems. AIP Conference Proceedings, 2005, , .	0.4	1
276	Crystallization and preliminary X-ray diffraction analysis of the lectin fromDioclea rostrataBenth seeds. Acta Crystallographica Section F: Structural Biology Communications, 2006, 62, 166-168.	0.7	1
277	High lattice temperature effects on the ultrafast electron transport in 4Hâ€SiC. Journal of Applied Physics, 2007, 102, 053710.	2.5	1
278	Dielectric function spectra from a nondegenerate polaron gas. Physics Letters, Section A: General, Atomic and Solid State Physics, 2007, 365, 478-482.	2.1	1
279	Band structure anisotropy effects on the ultrafast electron transport in 4H-SiC. Solid State Communications, 2008, 145, 397-400.	1.9	1
280	MOLECULAR FRACTIONATION WITH CONJUGATE CAPS STUDY OF THE INTERACTION OF THE ANACARDIC ACID WITH THE ACTIVE SITE OF TRYPANOSOMA CRUZI GAPDH ENZYME: A QUANTUM INVESTIGATION. Asian Journal of Pharmaceutical and Clinical Research, 2019, , 183-189.	0.3	1
281	Study of the vibrational properties of haloperidol under high-pressure. Vibrational Spectroscopy, 2020, 109, 103103.	2.2	1
282	Vibrational spectroscopy and phononâ€related properties of monoclinic GABA, a nonâ€proteinogenic inhibitory neurotransmitter amino acid. Journal of Raman Spectroscopy, 2021, 52, 1294-1307.	2.5	1
283	Exciton trapping in a periodically modulated magnetic field. Brazilian Journal of Physics, 2002, 32, 310-313.	1.4	1
284	A new analytical method for the calculation of the transmission coefficient of carriers through non-abrupt semiconductor heterostructures. Superlattices and Microstructures, 1993, 14, 221-226.	3.1	0
285	Ultrafast relaxation of hot minority carriers inpâ€GaAs. Journal of Applied Physics, 1993, 74, 2122-2124.	2.5	0
286	SURFACE PLASMONS ON UNIAXIAL CRYSTALS WITH GRATING SURFACES. Surface Review and Letters, 1996, 03, 1387-1392.	1.1	0
287	The influence of interfacial growth patterns on the transmission of electrons through nonabrupt GaAs/Al Ga1â^'As double-barriers. Microelectronic Engineering, 1998, 43-44, 371-375.	2.4	0
288	Resonances in GaAs/AlxGa1?xAs Heterojunctions Due to Si Shallow Donors Related Protrusions. Physica Status Solidi (B): Basic Research, 1998, 210, 683-687.	1.5	0

#	Article	IF	CITATIONS
289	Energy level broadening due to size fluctuation in quantum dots. Solid State Communications, 1998, 108, 803-807.	1.9	0
290	Interface-related band-bending effects on intersubband transitions in doped single quantum wells. Journal of Physics Condensed Matter, 1998, 10, 9681-9686.	1.8	0
291	Doping effects on the high-frequency mobility of minority carriers in p-GaAs. Journal of Applied Physics, 1998, 84, 1405-1407.	2.5	0
292	Interface-related restriction to potential depth estimates for single quantum wells. Journal of Physics Condensed Matter, 1999, 11, 1927-1934.	1.8	0
293	The effect of high Landau subbands filling on the hot-electron magneto-transport ultrafast transient in InSb. Physica B: Condensed Matter, 1999, 269, 28-33.	2.7	0
294	Smooth interface effects on the confinement properties of GaSb/AlxGa1â^'xSb quantum wells. Applied Surface Science, 2000, 166, 336-340.	6.1	0
295	High Temperature Effects on the Terahertz Mobility of Hot Electrons in 3C-SiC and 6H-SiC. Materials Science Forum, 2000, 338-342, 773-776.	0.3	0
296	AC hot carrier transport in 3C- and 6H-SiC in the terahertz frequency and high lattice temperature regime. Brazilian Journal of Physics, 2002, 32, 442-444.	1.4	0
297	Exciton Confinement in GaN/AlGaN Quantum Wells Enhanced by Non-Abrupt Interfaces. Physica Status Solidi (B): Basic Research, 2002, 234, 730-733.	1.5	0
298	Exciton stark shift in graded GaAs/AlxGa1â^'xAs quantum wells. Physica E: Low-Dimensional Systems and Nanostructures, 2003, 17, 220-221.	2.7	0
299	Lattice dynamic properties of interfaced InAs/GaAs superlattices. Physica E: Low-Dimensional Systems and Nanostructures, 2003, 17, 266-269.	2.7	0
300	Optical phonons dispersion relation in Si/3C-SiC heterostructures. Physica E: Low-Dimensional Systems and Nanostructures, 2003, 17, 270-271.	2.7	0
301	Numerical simulation of the optical properties of SiC/SiO2 quantum dots. Brazilian Journal of Physics, 2004, 34, 623-625.	1.4	0
302	Contribution of the charge image potential to carrier confinement in graded Si-based quantum wells. Brazilian Journal of Physics, 2004, 34, 684-686.	1.4	0
303	Concentration effects on the Raman scattering of AlGaN/GaN superlattices. Surface Science, 2004, 557, 73-79.	1.9	0
304	Conduction band anisotropy effects on the confined electron states of SiC/SiO2 quantum dots. Applied Surface Science, 2004, 237, 549-554.	6.1	0
305	Differences of Stark shift behavior in Si/SiO2 quantum wells and quantum dots. Applied Surface Science, 2004, 237, 544-548.	6.1	0
306	Si- and SiGe- high-k oxide nanostructures for optoelectronic devices. , 2005, , .		0

#	Article	IF	CITATIONS
307	Numerical simulation of Si1-xGex/HfO2/Si MOS devices. Physica Status Solidi C: Current Topics in Solid State Physics, 2005, 2, 2955-2957.	0.8	0
308	Excitons in type-I type-II strained Si/Si1-xGex graded quantum well. Physica Status Solidi C: Current Topics in Solid State Physics, 2005, 2, 2958-2961.	0.8	0
309	Exciton Confinement in Si/TiO2 0-2D Systems. AIP Conference Proceedings, 2005, , .	0.4	0
310	Stark Shift and Permanent Dipole Moment of Vertically Confined Excitons in InAs/GaAs Ring-Like Quantum Dots. AIP Conference Proceedings, 2005, , .	0.4	0
311	Anomalous Stark Effect in Intraband Absorption of Silicon Nanocrystals. AIP Conference Proceedings, 2005, , .	0.4	0
312	Remarkably Strong Image Potential Effects in SrTiO3/Si and HfO2/Si Tunneling Structures. AIP Conference Proceedings, 2005, , .	0.4	0
313	The Role of Non-abrupt Interfaces in SiC MOS Devices: Quantum Mechanical Simulations and Experiments. AIP Conference Proceedings, 2005, , .	0.4	0
314	Feasibility of IR-to-UV detection in SiC/SiO 2 heterostructures. , 2005, , .		0
315	Si-SiO2-Si and Si-CaCO3-Si core–double-shell nanoparticles: Tuning light emission from infrared to ultraviolet. Journal of Applied Physics, 2007, 102, 023712.	2.5	0
316	Consequences of nonstochiometric SiOx interfacial layers on the electrical characterization of metal-oxide-semiconductor devices. Journal of Applied Physics, 2007, 101, 034509.	2.5	0
317	262 Improved cytotoxic activity of Nor-β-lapachone-loaded PLGA microcapsules in PC3M prostate cancer cell line. European Journal of Cancer, 2014, 50, 87.	2.8	0
318	Interface effects on the vibrational properties of 3C-InN/3C-AlN superlattices. Brazilian Journal of Physics, 2002, 32, 445-447.	1.4	0
319	Quantum analysis/improvement of antipsychotic's docking results. FASEB Journal, 2013, 27, 810.9.	0.5	0